ICSV14

Cairns • Australia

9-12 July, 2007

14th International Congress on Sound & Vibration

PROPAGATION PHASE REPRESENTATION IN 3D SPACE USING POLES AND ZEROS IN COMPLEX FREQUENCY PLANE

Yoshinori Takahashi[1], Mikio Tohyama[2], and Kazunori Miyoshi[1]

[1]Kogakuin University, Tokyo, Japan

[2]Waseda University, Tokyo, Japan

takahashi@ieee.org (e-mail address of lead author)

Abstract

This paper describes the transfer function, including the coherent sound field, as the increased distance between source and observation points, from the point of view of the number of zeros in the complex frequency plane. The authors estimated the propagation phase obtained by linear regression analysis of the narrow-frequency-band phase characteristics of the minimum-phase component of the transfer function. The direct sound field estimated from the propagation phase of the minimum-phase characteristics consequently seems to be the coherent field within the critical distance. We determined that the zeros drift based on complex-integration analysis. When the sound source distance (SSD) increases, the zeros move toward a higher frequency; thus, an accumulated phase is produced following the propagation phase. When the SSD is long, even in the coherent field, we could confirm a pole-line around the theoretical value.

1. INTRODUCTION

Lyon [1, 2] clarified that the phase trend for the phase-frequency characteristics of a one-dimensional acoustic pipe is determined by phase delay according to the sound source distance (SSD), and he used the term propagation phase (PP) to express the phase delay. He also found the phase-frequency characteristics of the reverberation-sound field as a composition of PP indicated the phase delay obtained by direct sound and the reverberation phase (RP) obtained from reverberation sound. Lyon reported that PP could be observed from the phase-frequency-characteristic changes of the minimum-phase component in a two-dimensional or three-dimensional reverberant field, particularly since the transfer function of the acoustic pipe has minimum-phase characteristics. Lyon used this reasoning to clarify that the RP of a two-dimensional reverberation-sound field can be estimated from changes in the residue sign for poles of the transfer function, and found that RP can be estimated from the number of poles of the transfer function in regions where SSD r exceeds $kr = 2$ (k: wavenumber). The phase could express the poles and zeros used in the complex frequency plane. A pole makes phase return to π and a zero makes phase go to $-\pi$ in the minimum-phase component. Here, the poles are defined as the resonate characteristics of room reverberation. However, zeros change according to SSD. When SSD increases, zeros move toward high frequency; thus, accumulated phase is produced following propagation phase. Lyon called the movement of zeros ”zero drift”.

Takahashi and Tohyama [3] confirmed Lyon’s investigation by extracting PP and RP by using narrow-band linear-regression analysis of minimum-phase phase frequency characteristics and a distribution analysis of the zeros of the transfer function in the reverberation-sound field. Furthermore, Takahashi and Tohyama estimated the direct-sound field in a reverberant-sound field based on changes from PP to RP according to SSD, and compared it to the estimated value of the direct sound field based on wave theory [4], and to that of the critical distance defined from the energy ratio of direct sound to reverberant sound [5].

We determined that there was zero drift based on complex-integration analysis. When SSD increases, zeros move toward higher frequencies; thus, accumulated phase is produced following propagation phase. However, zero drift will cease when half the sampling frequency is reached. When SSD is long, even in a coherent field, we can confirm a pole-line around the theoretical value. If SSD is too short in a coherent field, we can no longer observe a pole-line. It is conceivable that direct sound is much greater than reverberation sound, and we therefore theoretically need an infinitely long impulse-response record.

The paper is organized as follows. Section 2 describes PP analysis, and explains PP extraction using narrow-band regression analysis of the minimum-phase phase spectrum. We determined that there was zero drift based on complex-integration analysis, which is discussed in Section 3. We confirmed there was a pole-line around the theoretical value when SSD is long, even in a coherent field, which is discussed in Section 4. Section 5 summarizes the paper.

2. PROPAGATION PHASE IN REVERBERANT ROOM

This section describes PP analysis [3]. We found that PP extraction requires decomposition of the transfer function into its minimum-phase and all-pass component, and we clarified that SSD information is included in the trend of the phase-frequency characteristics of the minimum-phase component (minimum-phase phase frequency characteristics) in the narrow-frequency band.

2.1 Measurement of impulse responses with SSD in echoic chamber

We measured impulse responses where SSDs, r, were set at 0.01, 0.02, 0.04, 0.08, 0.16, 0.32, 0.64, 1.28, and 2.56 m in a reverberation room with a volume of 183 m3 at a frequency of 48 kHz with 16-bit sampling. Figure 1(a) shows the measured impulse responses. We confirmed the arrival time of direct sound was delayed and the energy of D/R was decreased when SSD increased. The time delay in arrival was removed, and the phase propagation characteristics according to SSD were analyzed from impulse responses. Figure 1(b) shows a reverberation decay curve of impulse responses at the greatest distance (2.56 m) from the sound sources. We considered that there was sufficient S/N to measure impulse responses based on this reverberation decay curve.

2.2 PP analysis from minimum-phase component

Figure 2 has examples of minimum-phase phase frequency characteristics of impulse responses. Because the minimum-phase characteristics are such that the accumulated phase becomes 0, we were unable to find phase propagation according to SSD. Figure 3 has examples of the minimum-phase phase-frequency characteristics in the narrow-frequency band. We investigated how to extract PP using linear-regression analysis of these narrow-band phase-frequency characteristics [3].

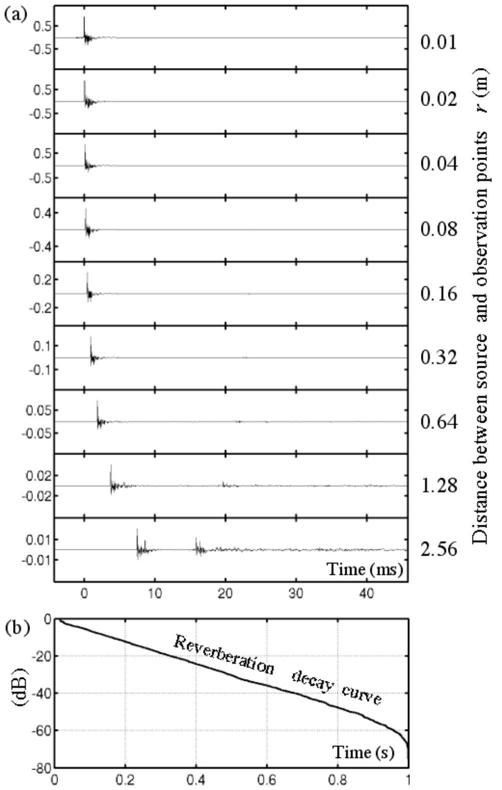

Figure 1. Impulse responses as distance between source and observation points r increases

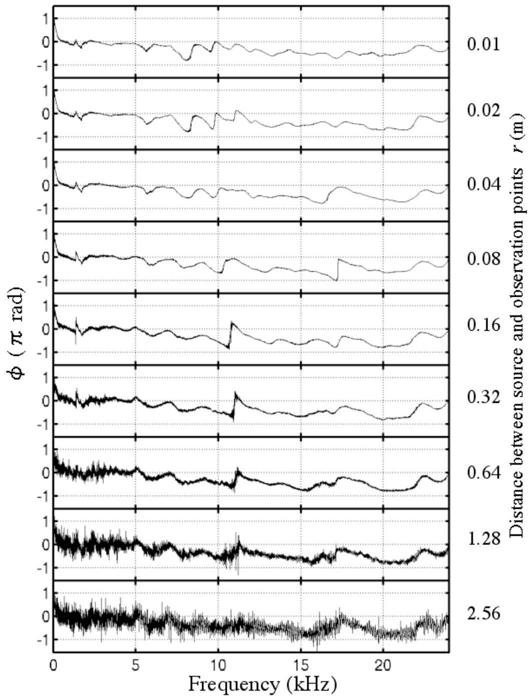

Figure 2. Samples of phase-frequency characteristics for minimum-phase components in room-transfer functions

Figure 4 outlines the process of extracting PP from the minimum-phase component of impulse responses. The steps are as follows. (1) Apply exponential decay-time windowing to measured impulse responses to extract impulse responses (reverberation time reaches about 1 s). (2) Analyze narrow-frequency band using band-pass filters. Set the center frequency, fc, to 100?1,000 Hz, and set each bandwidth to 200 Hz. (3) Subtract linear phase from the phase-frequency characteristics of the impulse responses in the narrow-frequency band. (4) Extract the phase-frequency characteristics of the minimum-phase component. (5) Normalize the phase-frequency characteristics to r_0 = 0.01 m. (6) Analyze the linear regression of phase-frequency characteristics against wavenumber k, and then analyze the trend. (7) Evaluate the change in the trend of the regression line according to SSD r.

Figure 5 shows linear-regression analysis of the minimum-phase phase-frequency characteristics against wavenumber k, where c is the speed of sound. We can see the gradient of

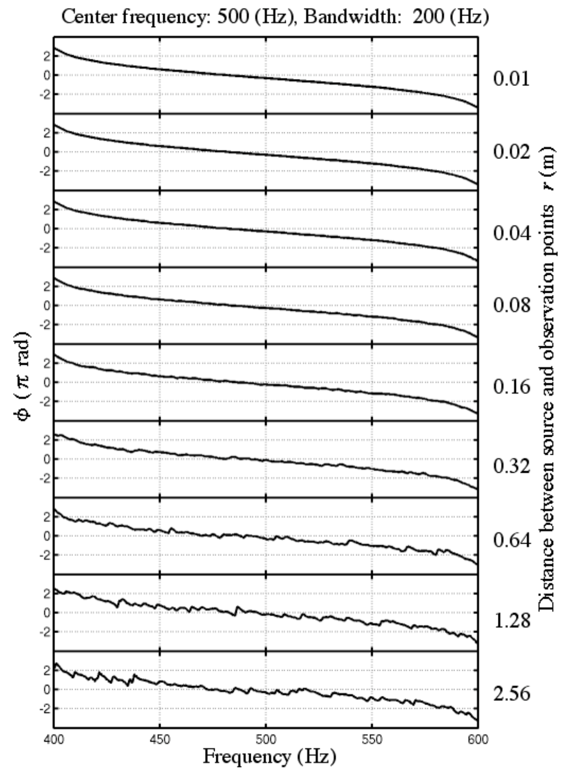

Figure 3. Records of narrow-band phase-frequency spectra for minimum-phase components

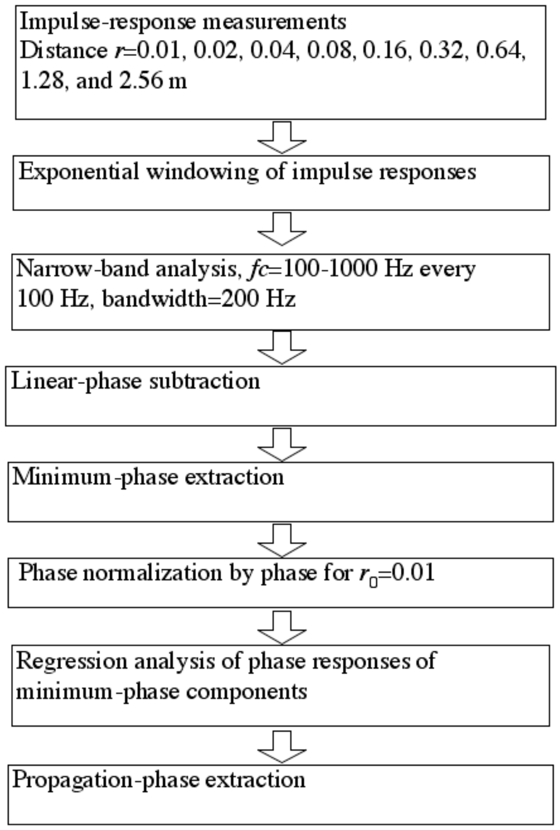

Figure 4. Procedure for extracting propagation phase from impulse-response records

the regression line increases along with increasing SSD, i.e., r. Figure 6 plots the results of evaluating the gradients of the regression lines with r. We can see the gradient of the regression line increases along with increasing r. The dotted line in this figure represents PP, i.e., r. The limit that can be considered the gradient of the phase-regression line in the minimum-phase component to be SSD (r) can be read as $r - r_0$ = 0.63 to 1.57 m.

2.3 Variance in deviation from PP in minimum-phase component

This section describes the variance in minimum-phase phase characteristics. We can not only see the gradient of the regression line increasing in Fig. 5, but also the variance in deviation from PP along with increasing r. Figure 7 has an evaluation of the variance in deviation from the PP of the minimum-phase phase-frequency characteristics using the variance in group delay obtained from Fig. 5. Variance in group delay does not depend on the frequency band, and is approximately constant. This corresponds to the results obtained by Tohyama, et al. [6] after analyzing group-delay variance.

2.4 SSD and phase-frequency characteristics including all-pass component

Figure 8 has an evaluation of the accumulated phase in the narrow-frequency band of the all-pass component due to changes in r. When SSD r is short, we can confirm PP in the all-pass

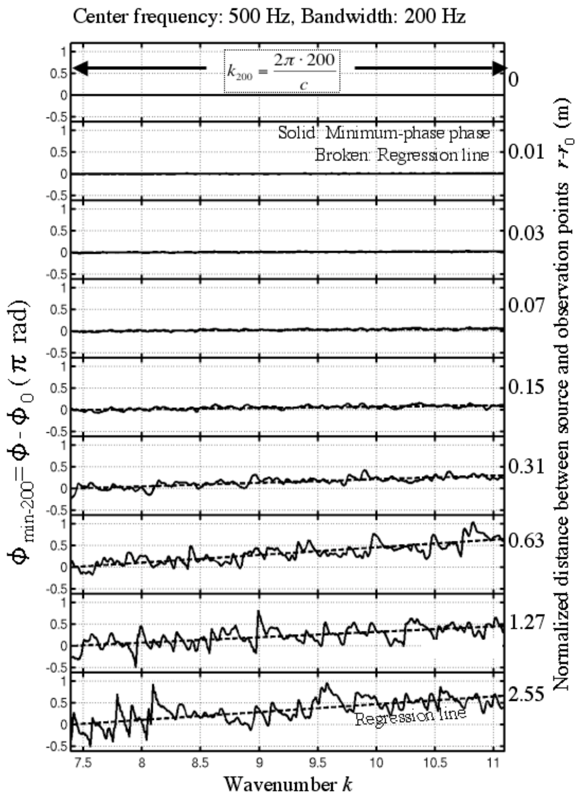

Figure 5. Linear-regression analysis of narrow-band minimum-phase phase characteristics

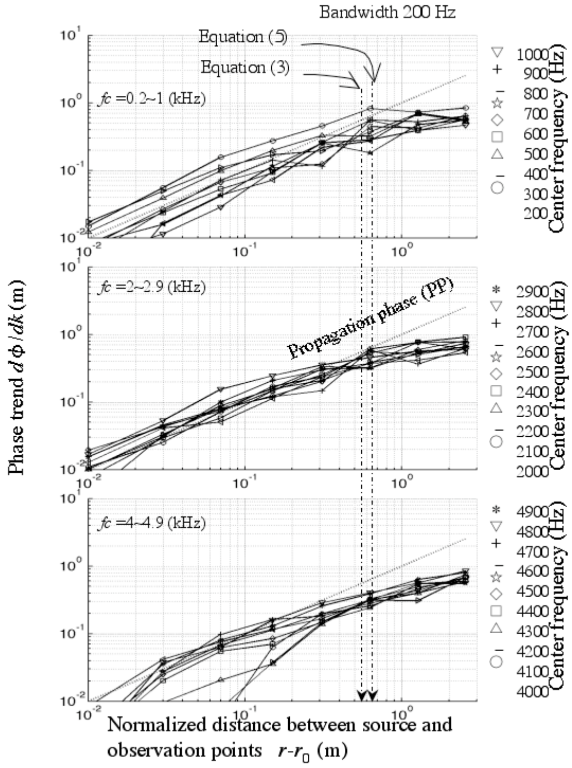

Figure 6. Slopes of regression lines in Fig. 5 against distance r between source and observation points

component in the same way as in the minimum-phase component. However, we confirmed that the PP field obtained from the all-pass component is smaller than that from the minimum-phase component. In addition, we could not confirm PP from the phase sum of the minimum-phase and all-pass components.

We can see from these results that it is important to divide the transfer function into its minimum-phase and all-pass components to extract the PP that Lyon investigated. We could confirm that the phase trend converges to a constant value around the phase of the all-pass component and the phase sum of the all-pass and minimum-phase components, according to SSD increases. This constant value is estimated as

$$\frac{\Phi_{ap200}}{k} \approx \tau \frac{d\omega}{dk} = 26.6(\mathrm{m}), \tag{1}$$

from the limit of the group-delay, $\tau = T_R/12.8$, for $T_R = 1$. We can see this from the solid line in Fig. 8 [6, 7].

2.5 Direct sound field

As discussed in Subsection 2.2, the limit that can be considered the gradient of the phase regression line in the minimum-phase component to be SSD (r) can be read as 0.63 to 1.57 m, as shown in Fig. 6. The coherent field described by Morse and Bolt [4] gives

$$r_{ph} = \sqrt{\frac{A}{64}}(\mathrm{m}). \tag{2}$$

where $A \approx 0.161V/T_R(\mathrm{m}^2)$, V is room volume (m^3), and T_R is the reverberation time (s). Here, the reverberation time is $1(\mathrm{s})$ and the room volume is $V = 183(\mathrm{m}^3)$ given as

$$r_{ph} = \sqrt{\frac{0.161 \times 183}{64 \times 1}} \approx 0.68(\mathrm{m}). \tag{3}$$

r_{ph} is indicted in Fig. 6 by the broken line.

The critical distance, r_c, based on the energy rate between direct sound and reverberant sound is defined by

$$\frac{I_0}{I_{rev}} = \frac{\bar{\alpha}S}{16\pi r_c^2} \equiv 1, \tag{4}$$

where I_0 means the intensity (W/m^2) of direct sound and I_{rev} is that of reverberant sound. Here, $\bar{\alpha}$ means the averaged absorption coefficient, and S means the surface area of the room (m^2). Consequently, the critical distance gives

$$r_c = \sqrt{\frac{\bar{\alpha}S}{16\pi}} \approx 0.1\sqrt{\frac{183}{\pi \times 1}} \approx 0.77(\mathrm{m}). \tag{5}$$

r_c is indicated in Fig. 6 by the dotted broken line. The direct sound field presumed from the PP of minimum-phase phase-frequency characteristics seems to correspond to the coherent field and critical distance.

3. Drifting Zeros and Propagation Phase

We will discuss the relationship between minimum-phase zeros and the propagation phase in this section.

3.1 Analysis of minimum-phase zeros by integrating complex contours

The difference in the numbers of poles and zeros on the unit circle of $H(z)$ is given by

$$N_P - N_z = -\frac{1}{2\pi i}\oint_c \frac{H'(z)}{H(z)}dz. \tag{6}$$

Here, $H(z)$ denotes the transfer function, $H'(z)$ is the derivative of the function, N_p is the number of poles, and N_z is the number of zeros. We calculated this complex-contour integration for each transfer function to analyze the difference in the numbers of poles and zeros. Figure 7 shows the contour of integrals in the complex frequency plane. The contour, c, is taken from inside the unit circle. The poles and zeros are included in the region surrounded by contour c. If we know the number of poles, then the result of this integration gives us the number of zeros. The number of poles can be estimated by the modal density of the average of the frequency interval of interest. Our impulse response record has a finite length. Therefore mathematically, the transfer function has no poles except for the origin of the complex-frequency domain. However, the integration results can be interpreted in terms of poles and zeros from the physical point of view, if the length of the impulse response record is sufficiently longer than the reverberation time.

3.2 Zero drift representation

Figure 8 shows the results obtained by analyzing complex integration. The horizontal axis represents frequency, the vertical axis is SSD, and the colors represent the number of differences between the poles and zeros obtained from complex-integration analysis. We can see zero drift from low to high frequencies. If we look at the low-frequency range, then large differences can be observed when SSD is short. However, if SSD increases these large differences are expanded into the high-frequency range.

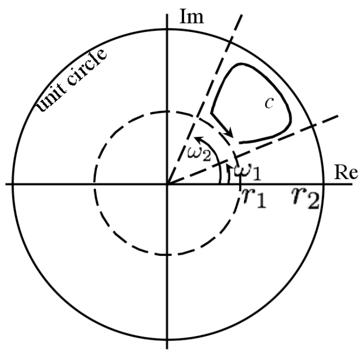

Figure 7. Contour of integrals in complex-frequency plane

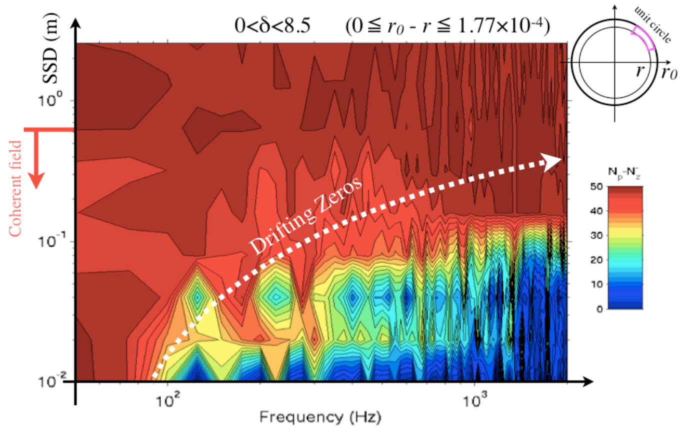

Figure 8. Zero drift display based on complex-contour-integration analysis

4. POLE LINE ANALYSIS

The poles are distributed on a line above the frequency axis in the complex-frequency domain as shown in Fig. 9. The pole line, which connects adjacent poles, is where the distance denoted by δ_0 from the real frequency axis can be determined by $\delta_0 \approx T_R/6.9$ with a reverberation time of T_R. The reverberation time in this experiment was 1 s on average; therefore, $\delta_0 \approx 7$.

Figure 10 shows the results for complex-contour-integration analysis, including the pole line.

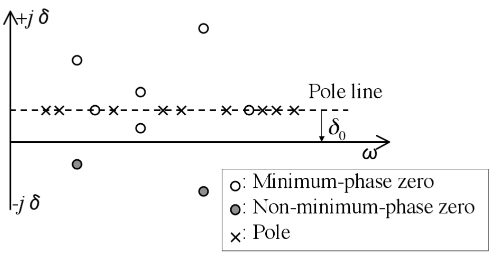

Figure 9. Schematic of poles, zeros, and pole-line

Each panel illustrates the numerical results on the difference $N_p - N_z$ corresponding to SSD. The horizontal axis represents the frequency, and the vertical axis is the distance from the real-frequency axis. The colors indicate numerical numbers. The high-density region can be interpreted to indicate the pole line. When SSD is long, even in the coherent field, we can confirm a pole line around $\delta \approx 7$. Theoretically, the poles do not move on the complex frequency plane, even if SSD changes. However, if SSD is too short in the coherent field, we can no longer observe a pole line. This is because direct sound is much greater than reverberation sound, and we therefore need a very long impulse response record. That is, we theoretically need one that is infinitely long.

5. CONCLUSION

This paper discussed the transfer function phase and zeros in a reverberation field. We confirmed the propagation phase by the linear-regression analysis of narrow-frequency-band phase characteristics for the minimum-phase component of the transfer function. Consequently, the direct-sound field presumed from the propagation phase of minimum-phase characteristics seems to be the coherent field within the critical distance. We then demonstrated zero drift based on complex-integration analysis. When SSD increases, zeros move toward high frequency; thus, an accumulated phase is produced following the propagation phase. When SSD is long, even in the coherent field, we could confirm a pole line around $\delta \approx 7$. If SSD is too short in the coherent field, we can no longer observe a pole line.

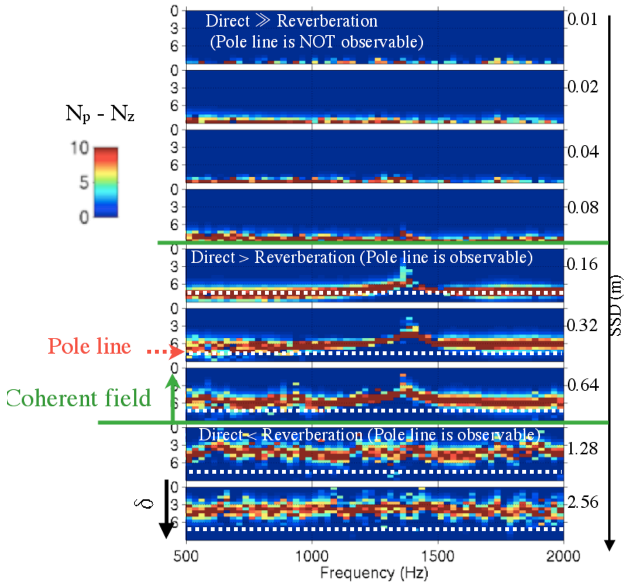

Figure 10. Pole-line display based on analysis of complex-contour integration

References

[1] R. Lyon, "Progressive phase trend in multi-degree-of-freedom systems", *Journal of the Acoustical Society of America* **73(4)**, 1223-1228 (1983).

[2] R. Lyon, "Range and frequency dependence of transfer function phase", *Journal of the Acoustical Society of America* **76(5)**, 1433-1437 (1984).

[3] Y. Takahashi, M. Tohyama, and Y. Yamasaki, "Phase responses of transfer functions and coherent field in a reverberation room", *IEICE Transactions on Fundamentals of Electronics, Communications and Computer Sciences* **Part 3, 90(4)**, 1-8 (2007). Japanese Edition: **J89-A(4)**, 291-297 (2006).

[4] P. Morse, and R. Bolt, "Sound waves in rooms", *Reviews of Modern Physics* **16**, 69-150 (1944).

[5] H. Kuttruff, "Sound in Enclosures", In M. J. Crocker (Ed), *Encyclopedia of Acoustics*, New York: J. Wiley, 1101-1114 (1997).

[6] M. Tohyama, and R. Lyon, "Phase variabilities and zeros in a reverberant transfer function", *Journal of the Acoustical Society of America* **95(1)**, 286-323 (1994).

[7] H. Kuttruff, *Room Acoustics 2nd ed. Applied Science*, London, 68 (1979).